A Novel Maximum Power Point Tracking Technique for Solar Panels Using a SEPIC or Cuk Converter

Henry Shu-Hung Chung, *Member, IEEE*, K. K. Tse, *Member, IEEE*, S. Y. Ron Hui, *Fellow, IEEE*, C. M. Mok, and M. T. Ho, *Student Member, IEEE*

***Abstract*—A novel technique for efficiently extracting the maximum output power from a solar panel under varying meteorological conditions is presented. The methodology is based on connecting a pulse-width-modulated (PWM) dc/dc SEPIC or Cuk converter between a solar panel and a load or battery bus. The converter operates in discontinuous capacitor voltage mode whilst its input current is continuous. By modulating a small-signal sinusoidal perturbation into the duty cycle of the main switch and comparing the maximum variation in the input voltage and the voltage stress of the main switch, the maximum power point (MPP) of the panel can be located. The nominal duty cycle of the main switch in the converter is adjusted to a value, so that the input resistance of the converter is equal to the equivalent output resistance of the solar panel at the MPP. This approach ensures maximum power transfer under all conditions without using microprocessors for calculation. Detailed mathematical derivations of the MPP tracking technique are included. The tracking capability of the proposed technique has been verified experimentally with a 10-W solar panel at different insolation (incident solar radiation) levels and under large-signal insolation level changes.**

***Index Terms*—dc-dc power conversion, maximum-power-point-tracking, photovoltaic.**

I. Introduction

SOLAR panel is the fundamental energy conversion component of photovoltaic (PV) systems [1], [2]. It has been used in many applications [3], such as aerospace industries, electric vehicles, communication equipment, etc. As the solar panels are relatively expensive, much research work has been conducted to improve the utilization of solar energy. Physically, the power supplied by the panels depends on many extrinsic factors, such as insolation (incident solar radiation) levels, temperature, and load condition. Thus, a solar panel is typically rated at an insolation level together with a specified temperature, such as 1000 W/m^2 at 25 °C. Its electrical power output usually increases linearly with the insolation and decreases with the cell/ambient temperature.

In practice, there are three possible approaches for maximizing the solar power extraction in medium- and large-scale PV systems. They are sun tracking, maximum power point (MPP) tracking or both. For the small-scale systems, the use of MPP tracking only is popular for economical reasons. In the last two decades, various methods including the power-matching scheme [4]–[6], curve-fitting technique [7], [8], perturb-and-observe method [9]–[14], and incremental conductance algorithm [15]–[17] have been proposed for tracking the MPP of solar panels.

The power-matching scheme requires the selected solar panels to have suitable output characteristics [4], [5] or configurations [6] that can be matched with particular loads. However, these techniques only approximate the location of the MPP because they are basically associated with specific insolation and load conditions [17].

The curve-fitting technique requires prior examination of the solar panel characteristics, so that an explicit mathematical function describing the output characteristics can be predetermined. The method proposed in [7] and [8] is based on fitting the operating characteristic of the panel to the loci of the MPP of the PV systems. Although this technique attempts to track the MPP without computing the voltage–current product explicitly for the panel power, the curve-fitting technique cannot predict the characteristics including other complex factors, such as aging, temperature, and a possible breakdown of individual cells [7].

The perturb-and-observe (PAO) method is an iterative approach that perturbs the operation point of the PV system, in order to find the direction of change for maximizing the power [9]–[12]. It is operated by periodically perturbing the panel terminal voltage and comparing the PV output power with that of the previous perturbation cycle. Maximum power control is achieved by forcing the derivative of the power to be equal to zero under power feedback control. This has an advantage of not requiring the solar panel characteristics. However, this approach is unsuitable for applications in rapidly changing atmospheric conditions [17]. The solar panel power is measured by multiplying its voltage and current, either with a microprocessor or with an analog multiplier [10]. In [13] and [14], the tracking technique is based on the fact that the terminal voltage of the solar panels at MPP is approximately at 76% of the open-circuit voltage. Thus, in order to locate the MPP, the panel is disconnected from the load momentarily so that the open-circuit voltage can be sampled and kept as reference for the control loop.

The disadvantage of the PAO method can be improved by comparing the instantaneous panel conductance with the incremental panel conductance [15]–[17]. This method is the most accurate one among the above methods and is usually

Manuscript received March 27, 2000; revised November 1, 2001. This work was supported by the City University of Hong Kong under Project 7001211 and the Research Grant Council of the Hong Kong Special Administrative Region, China, under Project CityU 1/00C. Recommended by Associate Editor Y.-F. Liu.

The authors are with the Department of Electronic and Communications Engineering, City University of Hong Kong, Kowloon Tong, Hong Kong.

Digital Object Identifier 10.1109/TPEL.2003.810841

named as the incremental conductance technique (ICT). The input impedance of a switching converter is adjusted to a value that can match the optimum impedance of the connected PV panel. This technique gives a good performance under rapidly changing conditions. The implementation is usually associated with a microcomputer [15] or digital signal processor [17].

Concluding the above discussions, one of the most desirable approaches of implementing a MPP tracker is to use the ICT without requiring sophisticated digital sampling or mathematical manipulations. Moreover, the realization should be of low-cost and high accuracy and control capability. In this paper, a novel technique for efficiently maximizing the output power of a solar panel supplying to a load or battery bus under varying meteorological conditions is presented. The proposed MPP tracking is achieved by connecting a pulse-width-modulated (PWM) dc/dc SEPIC or Cuk converter between a solar panel and a load or battery bus. The converter is operating in discontinuous capacitor voltage (DCV) mode whilst its input current is kept continuous. The nominal duty cycle of the main switch in the converter is adjusted to a certain value, so that the input resistance of the converter is equal to the equivalent output resistance of the solar panel. This ensures the maximum power transfer. By modulating a small-signal sinusoidal perturbation into the duty cycle of the main switch and comparing the maximum variation in the input voltage and the voltage stress of the main switch, the MPP of the panel can be located. The tracking capability of the proposed technique has been verified experimentally with a 10-W solar cell panel at different insolation (incident solar radiation) levels and temperatures and under different large-signal insolation changes.

II. Modeling of the Converter Input at MPP

A. Derivation of the Required Dynamic Input Characteristics of a Converter at MPP

Fig. 1 shows an equivalent circuit of the solar panel connecting to a converter. The equivalent circuit for solar panels generally consists a current source shunted by a diode and a resistor and with an output series resistor [18], [19]. However, a Thevenin's equivalent circuit is used to represent the solar panel at the MPP in this case. The solar panel is represented by a voltage source v_g connecting in series with an output resistance r_g. The input voltage and the equivalent input resistance of the converter are v_i and r_i, respectively. As the input power P_i to the converter is equal to the output power P_o of the solar panel

$$P_i = P_o = \frac{v_i^2}{r_i}. \tag{1}$$

The rate of change of P_i with respect to v_i and r_i can be shown to be

$$\partial P_i = 2\,\frac{v_i}{r_i}\,\partial v_i - \frac{v_i^2}{r_i^2}\,\partial r_i. \tag{2}$$

At the MPP, the rate of change of P_i equals zero. Hence

$$\partial P_i = 0 \quad \Rightarrow \quad \frac{\partial v_i}{\partial r_i} = \frac{V_i}{2R_i} \tag{3}$$

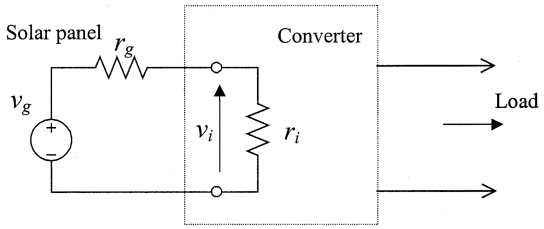

Fig. 1. Equivalent circuit of a solar panel connecting to a converter.

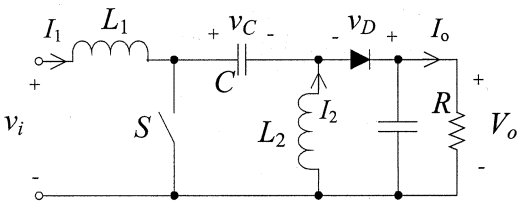

Fig. 2. Circuit diagram of a SEPIC converter.

where V_i and R_i are the input voltage and the input resistance at MPP.

The above equation gives the required dynamic input characteristics of the converter at the MPP. The input voltage will have a small-signal variation of δv_i if the input resistance is subject to a small-signal change of δr_i. That is

$$\frac{\delta v_i}{\delta r_i} \approx \frac{\partial v_i}{\partial r_i} = \frac{V_i}{2R_i}. \tag{4}$$

B. Input Resistance and Voltage Stress of a SEPIC Converter

Fig. 2 shows the circuit diagram of a SEPIC converter. If the converter is operated in DCV mode [20], there are in total three circuit topologies in one switching cycle. The sequence of operation and the waveforms are shown in Fig. 3. If the two inductor currents (i.e., I_1 and I_2) are assumed to be constant, the capacitor voltage $v_C(t)$ and diode voltage $v_D(t)$ in the respective three operating intervals can be expressed as

$$v_C(t) = \begin{cases} \dfrac{I_1(1-d)T_S}{C} - V_o - \dfrac{I_2}{C}\,t, & 0 < t < d_1T_S \\ -V_o, & d_1T_S < t < dT_S \\ \dfrac{I_1}{C}\,(t - dT_S) - V_o, & dT_S < t < T_S \end{cases} \tag{5a}$$

$$v_D(t) = \begin{cases} V_o + v_C(t), & 0 < t < d_1T_S \\ 0, & d_1T_S < t < T_S. \end{cases} \tag{5b}$$

As $v_C(d_1T_S) = -V_o$

$$\frac{I_1(1-d)T_S}{C} - V_o - \frac{I_2}{C}\,d_1T_S = -V_o$$

$$\Rightarrow \qquad d_1 = \frac{I_1}{I_2}\,(1-d). \tag{6}$$

Under the steady-state condition, the average voltage across L_2 is zero. Hence, the V_o is equal to the average value of v_D. That is

$$V_o = \frac{1}{T_S}\int_0^{D_1T_S} v_D(t)dt = \frac{T_S}{2C}\,I_1(1-d)d_1. \tag{7}$$

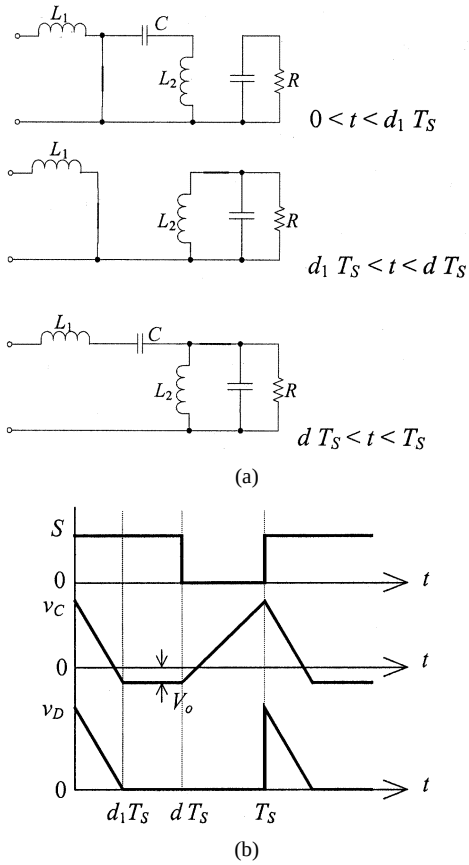

Fig. 3. Principles of operation. (a) Topology sequence. (b) Theoretical waveforms of v_C and v_D.

As the average voltage across L_1 is also zero

$$v_i = \frac{1}{T_S}\int_0^{T_S} v_C(t)dt = \frac{T_S}{2C} I_1(1-d)^2. \tag{8}$$

Hence, the input resistance r_i of the converter is

$$r_i = \frac{v_i}{I_1} = \frac{(1-d)^2}{2Cf_S} \tag{9}$$

where $f_S = 1/T_S$ is the switching frequency.

Moreover, the voltage stress across the main switch S v_{stress}, equals

$$v_{\text{stress}} = v_C(T_S) + V_o = \frac{I_1}{C}(1-d)T_S = \frac{2}{1-d} v_i. \tag{10}$$

In the proposed technique, (9) and (10) will be used to locate the MPP of a solar panel. As shown in [21], the input resistance and the voltage stress across the main switch of a Cuk converter is same as (9) and (10), respectively. Hence, both SEPIC and Cuk converters exhibit similar r_i and v_{stress}, and thus, they can be used to locate the MPP.

C. Dynamic Input Resistance of the Converter Under Perturbation

If a small-signal sinusoidal perturbation δd is injected into d

$$d = D + \delta d = D + \hat{d}\sin\omega t \tag{11}$$

where $\omega = 2\pi f$, and D is the nominal duty cycle at the MPP, and $\hat{d}$ and f are the amplitude and frequency of the injected perturbation, respectively. In the following derivations, the value of f is assumed to be much smaller than f_S.

By substituting (11) into (9), the input resistance can be expressed as

$$r_i = \frac{(1-D)^2}{2f_SC} - \frac{(1-D)}{f_SC}\hat{d}\sin\omega t + \frac{1}{2f_SC}\hat{d}^2\sin^2\omega t. \tag{12}$$

Hence, r_i includes two main components, namely, the static resistance R_i at the MPP and the dynamic resistance δr_i around the MPP. Each one can be expressed as

$$R_i = \frac{(1-D)^2}{2f_SC} \tag{13}$$

and

$$\delta r_i = -\frac{(1-D)}{f_SC}\hat{d}\sin\omega t + \frac{1}{2f_SC}\hat{d}^2\sin^2\omega t. \tag{14}$$

By substituting (14) into (4), the input voltage variation δv_i at the MPP can be expressed as

$$\delta v_i = \delta\overline{v}_i + \delta\tilde{v}_i \quad \text{and} \quad \delta\tilde{v}_i = \delta\tilde{v}_{i,1} + \delta\tilde{v}_{i,2} \tag{15}$$

where $\delta\overline{v}_i = (V_i/(4(1-D)^2))\,\hat{d}^2$, $\delta\tilde{v}_{i,1} = -(V_i/(1-D))\,\hat{d}\sin\omega t$, and $\delta\tilde{v}_{i,2} = -(V_i/(4(1-D)^2))\,\hat{d}^2\cos 2\omega t$.

δv_i is maximum when

$$\omega t = \frac{(2n+1)}{2}\pi, \qquad n = 1, 3, 5, \ldots. \tag{16}$$

Its maximum value $\delta v_{i,\max}$ can be shown to be equal to

$$\delta v_{i,\max} = \frac{V_i}{(1-D)}\hat{d} + \frac{V_i}{2(1-D)^2}\hat{d}^2. \tag{17}$$

Considering the ac-component of δv_i, its maximum value $\delta\tilde{v}_{i,\max}$ can be expressed as

$$\delta\tilde{v}_{i,\max} = \delta\tilde{v}_{i,m1} + \delta\tilde{v}_{i,m2} \tag{18}$$

where $\delta\tilde{v}_{i,m1} = (V_i/(1-D))\,\hat{d}$, and $\delta\tilde{v}_{i,m2} = (V_i/(4(1-D)^2))\,\hat{d}^2$.

The ratio between the magnitude of $\delta\tilde{v}_{i,m1}$ and $\delta\tilde{v}_{i,m2}$ $\Re$ is

$$\Re = \left|\frac{\delta\tilde{v}_{i,m2}}{\delta\tilde{v}_{i,m1}}\right| = \frac{\hat{d}}{4(1-D)}. \tag{19}$$

$\Re$ is an index showing the spectral quality of the input voltage variation at the frequency of the injected perturbation with respect to the amplitude of the perturbation. The smaller the value of $\Re$, the more dominant the component of the injected frequency in δv_i will be.

D. Voltage Stress of the Main Switch Under Perturbation

The maximum value of v_{stress} (i.e., $v_{\text{stress},\max}$) under a sinusoidal perturbation can be obtained by substituting $d = D + \delta d$

and $v_i = V_i + \delta v_i$ into (10). Thus

$$\begin{aligned} v_{\text{stress}} &= \frac{2}{(1-D-\delta d)}(V_i+\delta v_i) \\ &= \frac{2}{(1-D)}\frac{1}{1-\frac{\delta d}{(1-D)}}(V_i+\delta v_i) \\ &= \frac{2}{(1-D)}\left[1+\frac{1}{(1-D)}\delta d+\frac{1}{(1-D)^2}\delta d^2+\cdots\right] \\ &\quad \cdot (V_i+\delta v_i) \\ &= \frac{2}{(1-D)}V_i+\frac{2\delta d}{(1-D)^2}\left(\frac{1}{1-\frac{\delta d}{1-D}}\right) \\ &\quad \cdot (V_i+\delta v_i)+\frac{2}{1-D}\delta v_i \\ &= V_{\text{stress}}+\delta v_{\text{stress}} \end{aligned} \tag{20}$$

where $V_{\text{stress}} = (2V_i/(1-D))$ and

$$\delta v_{\text{stress}} = \frac{2\delta d}{(1-D)^2}\left(\frac{1}{1-\frac{\delta d}{1-D}}\right)(V_i+\delta v_i)+\frac{2}{1-D}\delta v_i.$$

The maximum value of v_{stress}, $v_{\text{stress, max}}$, can be approximated by substituting $\delta d = \hat{d}$ and $\delta v_i = \delta v_{i,\max}$ in (17) into (18). It can be shown that

$$v_{\text{stress, max}} = \frac{2V_i}{(1-D)}\left[1+\varepsilon(D)\right] \tag{21}$$

where

$$\varepsilon(D) = \frac{2\hat{d}\left(1-D+\frac{\hat{d}}{4}\right)}{(1-D)(1-D-\hat{d})}.$$

Comparing (18) and (21), it can be shown that

$$\begin{aligned} \delta\tilde{v}_{i,\max} &= \beta v_{\text{stress, max}} \\ \beta &= \frac{\hat{d}}{2}\left[\frac{(1-D-\hat{d})\left(1-D+\frac{\hat{d}}{4}\right)}{(1-D)^2+\hat{d}\left(1-D+\frac{\hat{d}}{2}\right)}\right] \end{aligned} \tag{22}$$

at the MPP. If $\hat{d} \ll 1-D$, $\beta \cong \hat{d}/2$. Thus, $\delta\tilde{v}_{i,\max}$ and $v_{\text{stress, max}}$ form a relatively constant ratio of β at the MPP.

The control mechanism for locating the MPP is illustrated in Fig. 4. First, the error amplifier compares the maximum input ripple voltage (i.e., $\delta\tilde{v}_{i,\max}$) and the attenuated switch voltage stress (i.e., $\beta' v_{\text{stress, max}}$) and generates an error signal. Theoretically, β' should be equal to β in (22). However, as β is dependent on D, a constant value is used to represent it for the sake of simplicity in the implementation. Its value is equal to $r_2/(r_1+r_2)$ so that

$$\beta' = \frac{r_2}{r_1+r_2} = \frac{1}{D_{\max}-D_{\min}}\int_{D_{\min}}^{D_{\max}}\beta(D)\,dD \tag{23}$$

where $D_{\min}$ and $D_{\max}$ are the minimum and maximum duty cycle of the main switch, respectively.

$D_{\max}$ is determined by the minimum input resistance $R_{i,\min}$ of the converter, which is also the minimum equivalent output resistance of the solar panel. By using (9)

$$D_{\max} = 1-\sqrt{2R_{i,\min}Cf_S}. \tag{24}$$

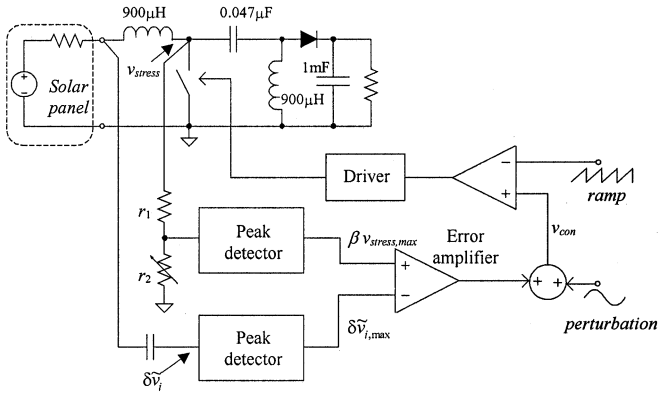

Fig. 4. Block diagram of the proposed MPP tracking method.

For the converter operating in DCV mode, we must ensure that $d_1 \le d$. The output current I_o can be expressed as

$$\begin{aligned} I_o &= \frac{V_o}{R} = (1-d)I_1+(1-d_1)I_2 \\ \Rightarrow \quad I_2 &= \frac{1}{1-d_1}\left[\frac{V_o}{R}-(1-d)I_1\right]. \end{aligned} \tag{25}$$

d_1 is determined by substituting (6) and (7) into (25), and thus

$$D_{\min} = \sqrt{2RCf_S}. \tag{26}$$

Second, the error signal is superimposed with a small-signal sinusoidal perturbation. Third, the combined signal v_{con} is compared to a ramp function to generate a PWM gate signal to the main switch.

The tracking action can be illustrated by considering the values of $\delta\tilde{v}_{i,\max}$ and $v_{\text{stress, max}}$ when d does not equal D. Based on Fig. 1 and using (9), it can be shown that

$$\begin{aligned} v_i &= \frac{r_i}{r_i+r_g}v_g \\ \Rightarrow \quad \delta v_i &= -\frac{2r_i r_g}{(r_i+r_g)^2}\frac{v_g}{(1-d)}\delta d. \end{aligned} \tag{27}$$

Thus

$$\delta\tilde{v}_{i,\max} = \frac{2\alpha}{(1+\alpha)^2}\frac{v_g}{(1-d)}\hat{d} \tag{28}$$

where $\alpha = r_i/r_g = [(1-d)/(1-D)]^2$.

By substituting (27) and (28) into (20), $v_{\text{stress, max}}$ is equal to

$$v_{\text{stress, max}} = \frac{2\alpha\left[(1+\alpha)(1-d)+2\hat{d}\right]}{(1-d)(1-d-\hat{d})(1+\alpha)^2}v_g. \tag{29}$$

Referring to (22), if $\hat{d} \ll 1-d$, $\beta' \cong \hat{d}/2$. It can be shown that

$$\begin{aligned} \Phi = \frac{\beta' v_{\text{stress, max}}}{\delta v_{i,\max}} &\cong \frac{1}{2}\left[\frac{(1+\alpha)(1-d)+2\hat{d}}{1-d-\hat{d}}\right] \\ &\cong \frac{1}{2}(1+\alpha) = \frac{1}{2}\left[1+\left(\frac{1-d}{1-D}\right)^2\right]. \end{aligned} \tag{30}$$

When r_i equals r_g (i.e., $\alpha = 1$), Φ becomes unity. This is the condition when the converter is at the MPP. If d is smaller than D, r_i will be larger than r_g (i.e., $\alpha > 1$), and Φ becomes larger than unity. The error amplifier will then generate a signal so as

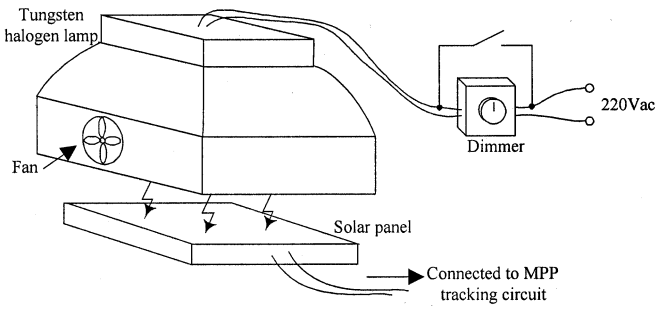

Fig. 5. Experimental setup of the solar panel for testing the proposed MPP tracking technique.

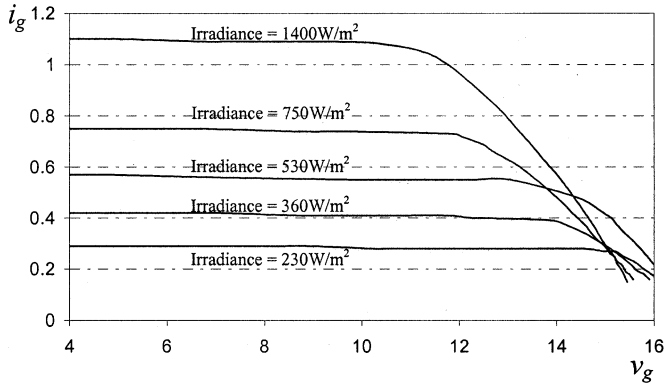

(a)

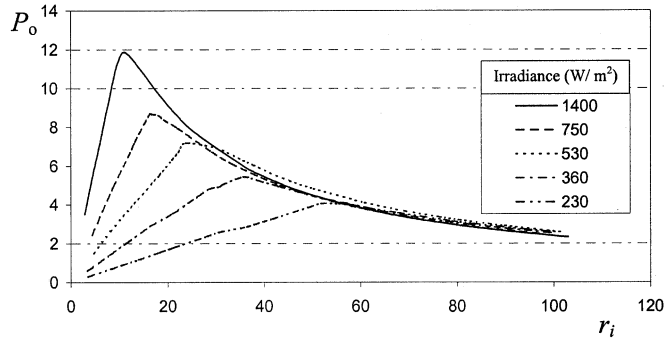

(b)

Fig. 6. Solar panel characteristics at different P_{lamp}. (a) i_g versus v_g. (b) P_o versus r_i.

to increase the duty cycle. Conversely, if d is larger than D, r_i will be smaller than r_g (i.e., $\alpha < 1$). Φ becomes less than unity. The error amplifier will then generate a signal so as to decrease the duty cycle. The above regulatory actions cause the feedback network to adjust the duty cycle, in order to make $\Phi = 1$ or $r_i = r_g$.

III. Experimental Verifications

A control experiment has been performed using a solar panel Siemens SM-10 with a rated output power of 10 W. The setup is shown in Fig. 5 and the component values of the SEPIC converter are shown in Fig. 4. The output resistance R equals 10 Ω. The switching frequency is set at 80 kHz, and the injected sinusoidal perturbation frequency is 500 Hz. The radiation level illuminated on the solar panel is adjusted by controlling

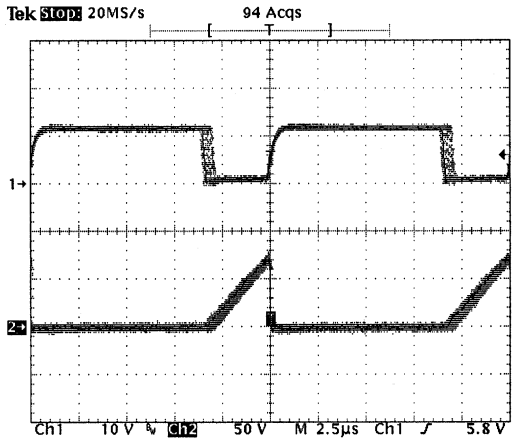

(a)

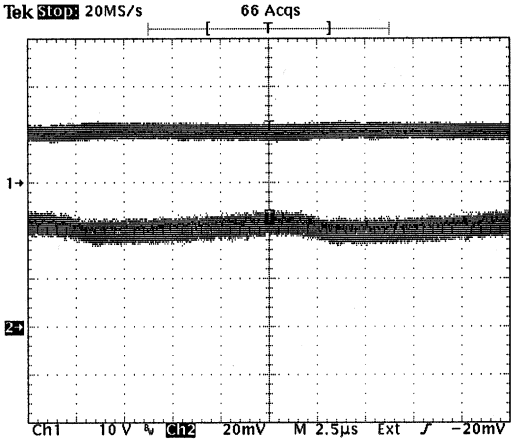

(b)

Fig. 7. Detailed experimental waveforms of the SEPIC converter. (a) Ch1: gate signal, 10 V/div; Ch2: switch voltage stress, 50 V/div. (b) Ch1: input voltage, 10 V/div; Ch2: input current, 0.5 A/div.

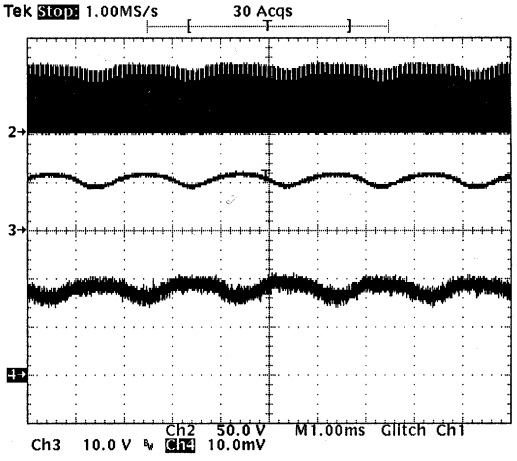

Fig. 8. Macroscopic view of the experimental waveforms of the SEPIC converter. Ch2: switch voltage stress, 50 V/div; Ch3: input voltage, 10 V/div; Ch4: input current, 0.5 A/div.

the power of a 900 W halogen lamp using a light dimmer. The bypass switch is used to give the maximum brightness from the lamp for studying the transient response. The surface temperature of the panel is maintained at about 40 °C. The measured $v_g - i_g$ characteristics and the output power versus

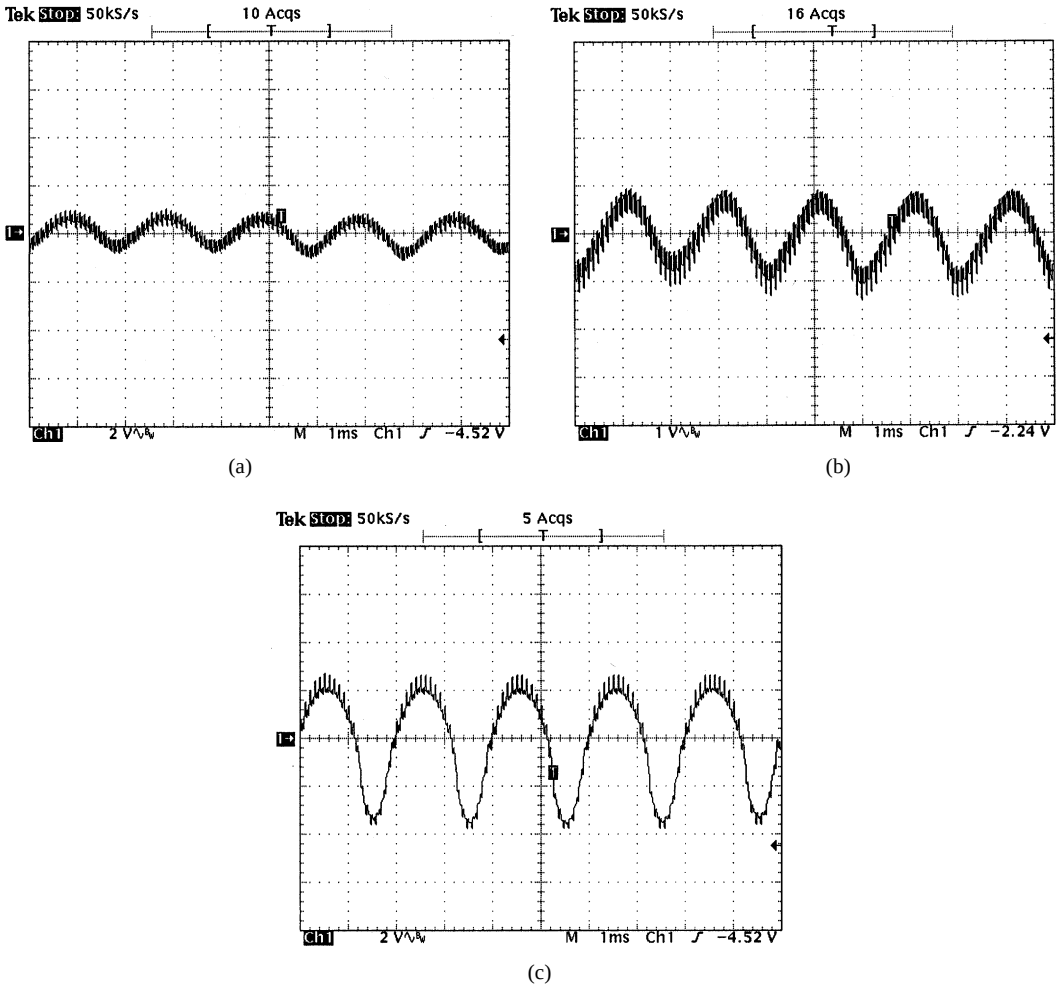

Fig. 9. Experimental waveforms of $\delta\bar{v}_i$ with respect to different value of $\Re$. (a) $\Re = 0.02$. (b) $\Re = 0.05$. (c) $\Re = 0.1$.

the terminal resistance of the solar panel at different insolation levels are shown in Fig. 6(a) and (b), respectively. Under a given insolation level, it can be seen that the panel output power will be at its maximum under a specific value of the terminal resistance. When the irradiance is 1400 W/m^2, the required terminal resistance is 14 Ω, in order to extract maximum power from the solar panel. Thus, by applying (24) and (26), $D_{\min}$ and $D_{\max}$ equal 0.274 and 0.675, respectively. Based on (9), the variation of the input resistance is between 14 and 70 Ω, which is well within the required tracking range of the input resistance shown in Fig. 6(b).

Detailed experimental waveforms of the gate signal, the switch voltage stress, the converter input terminal voltage, and the input inductor current in one switching cycle at the maximum lamp power are shown in Fig. 7. Macroscopic views of the switch voltage stress, input voltage, and input current are shown in Fig. 8. It can be seen that a low-frequency variation of 500 Hz is superimposed on all waveforms. They are all in close agreement with the theoretical ones. In addition, the input current is continuous. Thus, the proposed MPP tracker is better than the one using classical buck-type converter [1], which takes pulsating input current. Moreover, it is unnecessary to interrupt the system, in order to test the open-circuit terminal voltage of the solar panel as in [13] and [14].

Fig. 9 shows the ac-component of the converter input terminal voltage with $\Re$ equal to 0.02, 0.05, and 0.1, respectively. As $\Re$ increases, the ac-component will be distorted because the second-order harmonics become dominant in (15).

In order to observe the feedback action of the proposed approach under a large-signal variation in the radiation level from 360 to 1400 W/m^2. The transient waveform of the feedback signal is shown in Fig. 10. The settling time is about 0.4 s. Based on the results in Fig. 6(b), a comparison of the maximum extractable power from the solar panel and the measured output power with the proposed control scheme under different insolation levels is shown in Fig. 11. It can be seen that the proposed control technique can track the output power of the panel with an error of less than 0.2 W. A major reason for the discrepancy is due to the variation of β with respect to the duty cycle shown in (23), which will directly affect the tracking accuracy.

IV. Conclusion

A novel technique using a SEPIC or Cuk converter to efficiently track the MPP of a solar panel has been presented. The technique is simple and elegant and does not require complicated mathematical computation, hardware implementation,

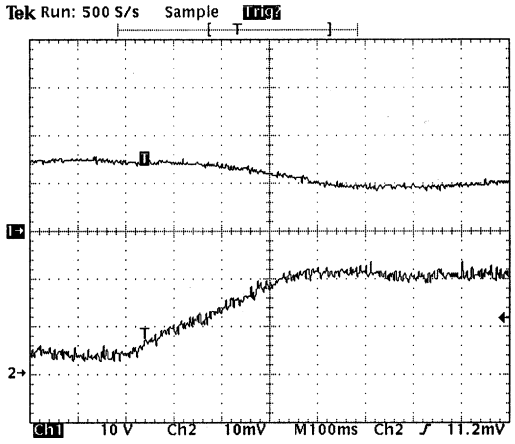

Fig. 10. Transient waveforms of the SEPIC converter when $P_{\rm lamp}$ is subject to a change from 500 to 900 W. Ch1: input voltage, 10 V/div. Ch2: input current, 0.5 A/div.

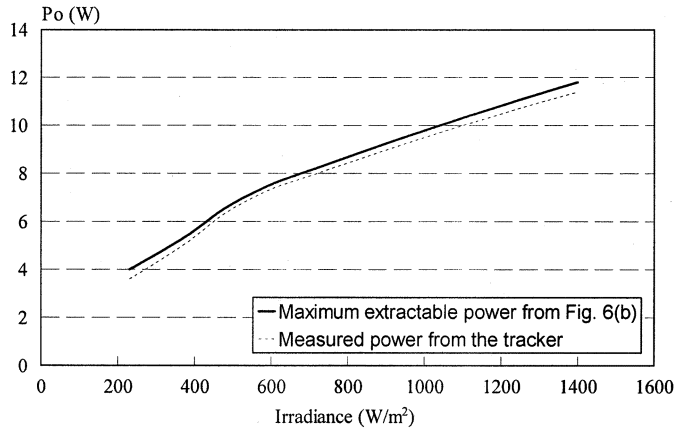

Fig. 11. Comparison of maximum solar panel output power using the proposed method and the maximum extractable value in Fig. 6(b) under different insolation.

microprocessor, or digital signal processor. The tracking capability of the proposed technique has been verified experimentally with a 10-W solar panel at different radiation levels. Compared to many existing methods, the proposed technique is unnecessary to

1) perform digital sampling of the converter parameters;
2) perform sophisticated mathematical computations of the panel output power;
3) approximate the panel output characteristics.

Hence, it can be used under a wide range of meteorological conditions. We have applied for a U.S. patent for this technique [22].

REFERENCES

[1] T. Markvart, *Solar Electricity*. New York: Wiley, 1994.
[2] M. Sharon *et al.*, "Solar rechargeable battery," *Electrochem. Acts*, vol. 36, no. 7, pp. 1107–1126, 1991.
[3] J. Schaefer, "Review of photovoltaic power plant performance and economics," *IEEE Trans. Energy Conv.*, vol. EC-5, pp. 232–238, June 1990.
[4] J. Applebaum, "The quality of load matching in a direct-coupling photovoltaic system," *IEEE Trans. Energy Conv.*, vol. 21, pp. 534–541, Dec. 1987.
[5] K. Khouzam, "Optimum load matching in direct-coupled photovoltaic power systems—Application to resistive loads," *IEEE Trans. Energy Conv.*, vol. 5, pp. 265–271, June 1990.
[6] A. Braunstein and Z. Zinger, "On the dynamic optimal coupling of a solar cell array to a load and storage batteries," *IEEE Trans. Power Apparat. Syst.*, vol. PAS-100, pp. 1183–1188, Mar. 1981.
[7] A. Kislovski and R. Redl, "Maximum-power-tracking using positive feedback," in *Proc. IEEE Power Electron. Spec. Conf.*, 1994, pp. 1065–1068.
[8] S. Wolf and J. Enslin, "Economical, PV maximum power point tracking regulator with simplistic controller," in *Proc. IEEE Power Electron. Spec. Conf.*, 1993, pp. 581–587.
[9] Z. Salameh and D. Taylor, "Step-up maximum power point tracker for photovoltaic arrays," *Solar Energy*, vol. 44, no. 1, pp. 57–61, 1990.
[10] M. G. Simoes and N. N. Franceschetti, "A RISC-microcontroller based photovoltaic system for illumination applications," in *Proc. IEEE Appl. Power Electron. Conf. Expo*, 2000, pp. 1151–1156.
[11] C. Sullivan and M. Powers, "A high-efficiency maximum power point tracker for photovoltaic arrays in a solar-powered race vehicle," in *Proc. IEEE Power Electron. Spec. Conf.*, 1993, pp. 574–580.
[12] J. Gow and C. Manning, "Controller arrangement for boost converter systems sourced from solar photovoltaic arrays or other maximum power sources," *Proc. Inst. Elect. Eng.*, vol. 147, no. 1, pp. 15–20, Jan. 2000.
[13] J. Enslin, M. Wolf, D. Snyman, and W. Swieger, "Integrated photovoltaic maximum power point tracking converter," *IEEE Trans. Ind. Electron.*, vol. 44, pp. 769–773, Dec. 1997.
[14] J. Schoeman and J. van Wyk, "A simplified maximal power controller for terrestrial photovoltaic panel arrays," in *Proc. IEEE Power Electron. Spec. Conf.*, 1982, pp. 361–367.
[15] A. Nafeh, F. Fahmy, O. Mahgoub, and E. Abou El-Zahab, "Microprocessor control system for maximum power operation of PV arrays," *Int. J. Numer. Model.*, vol. 12, pp. 187–195, 1999.
[16] O. Wasynzczuk, "Dynamic behavior of a class of photovoltaic power systems," *IEEE Trans. Power Apparat. Syst.*, vol. PAS-102, pp. 3031–3037, Sept. 1983.
[17] K. Hussein, I. Muta, T. Hoshino, and M. Osakada, "Maximum photovoltaic power tracking: An algorithm for rapidly changing atmosphere conditions," *Proc. Inst. Elect. Eng. G*, vol. 142, pp. 59–64, Jan. 1995.
[18] J. Merten, J. Asensi, C. Voz, A. Shah, R. Platz, and J. Andreu, "Improved equivalent circuit and analytical model for amorphous silicon solar cells and modules," *IEEE Trans. Electron Dev.*, vol. 45, pp. 423–429, Feb. 1998.
[19] U. Stutenbaeumer and B. Mesfin, "Equivalent model of monocrystalline, polycrystalline and amorphous silicon solar cells," *Renewable Energy*, vol. 18, pp. 501–512, 1999.
[20] D. Maksimovic and S. Cuk, "A unified analysis of PWM converters in discontinuous modes," *IEEE Trans. Power Electron.*, vol. 6, pp. 476–490, Mar. 1991.
[21] B. Lin and Y. Lee, "Power-factor correction using Cuk converters in discontinuous-capacitor-voltage mode operation," *IEEE Trans. Ind. Electron.*, vol. 44, pp. 648–653, Oct. 1997.
[22] H. Chung, K. K. Tse, and S. Y. R. Hui, "A novel maximum power tracking technique for solar panels," U.S. Patent (Pending).

Henry Shu-hung Chung (S'92–M'95) received the B.Eng. (with first class honors) degree in electrical engineering and the Ph.D. degree from The Hong Kong Polytechnic University, Hong Kong, in 1991 and 1994, respectively.

Since 1995, he has been with the City University of Hong Kong, where he is currently an Associate Professor in the Department of Electronic Engineering. His research interests include time-domain and frequency-domain analysis of power electronic circuits, switched-capacitor-based converters, random-switching techniques, digital audio amplifiers, soft-switching converters, and electronic ballast design. He has authored four research book chapters and over 140 technical papers including 70 refereed journal papers in the current research area and holds three U.S. patents.

Dr. Chung received the Grand Applied Research Excellence Award from the City University of Hong Kong in 2001. He is currently IEEE Student Branch Counselor and was Track Chair of the Technical Committee on Power Electronics Circuits and Power Systems, IEEE Circuits and Systems Society, from 1997 to 1998. He is presently an Associate Editor of the IEEE TRANSACTIONS ON CIRCUITS AND SYSTEMS I.

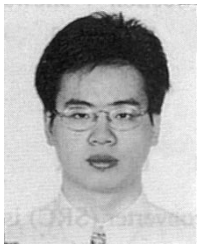

K. K. Tse received the B.Eng. (with honors) degree in electrical engineering from The Hong Kong Polytechnic University, in 1995 and the Ph.D. degree from the City University of Hong Kong in 2000.

He served as a Lecturer with the Institute of Vocational Education, Tsing Yi (formerly Technical College), Hong Kong, in 1998. From 1999 to 2001, He was a Research Fellow with the Electronic Engineering Department, City University of Hong Kong. Since June 2001, He has been with Johnson Electric, Hong Kong, where he is currently a Technical Specialist in R&D. He has published over 20 technical papers in the areas of his research interests, which include new numerical model methods and computer-aided simulation techniques, EMI reduction using random switching schemes for dc–dc converters, and new maximum power tracking technique for PV cells.

Dr. Tse received the First Prize from the IEEE Postgraduate Student Paper Contest, Hong Kong Section in 1998, the Third Prize Region 10 IEEE Postgraduate Student Paper Contest, in 1999, the Croucher Foundation Fellowship in 2000, and the Silver Award from the Young Inventor Competition in December 2000.

S. Y. (Ron) Hui (SM'94–F'03) was born in Hong Kong in 1961. He received the B.Sc degree (with honors) from the University of Birmingham, Birmingham, U.K., in 1984 and the D.I.C. and Ph.D. degrees from the Imperial College of Science and Technology, University of London, London, U.K., in 1987.

He was a Lecturer in power electronics at the University of Nottingham, Nottingham, U.K., from 1987 to 1990. In 1990, he went to Australia and took up a lectureship at the University of Technology, Sydney, where he became a Senior Lecturer in 1991. He joined the University of Sydney in 1993 and was promoted to Reader of electrical engineering and Director of the Power Electronics and Drives Research Group in 1996. Presently, he is a Chair Professor of electronic engineering and an Associate Dean of the Faculty of Science and Engineering at the City University of Hong Kong. He has published over 150 technical papers, including over 80 refereed journal publications. His research interests include all aspects of power electronics.

Dr. Hui received the Teaching Excellence Award in 1999 and the Grand Applied Research Excellence Award in 2001 from the City University of Hong Kong. He was appointed an Honorary Professor by the University of Sydney in 2000.

C. M. Mok was born in Hong Kong. He received the B.Eng. degree in electronic engineering from the City University of Hong Kong in 2000.

M. T. Ho (S'02) was born in Hong Kong in 1979. He received the B.Eng. (with first class honors) degree in electronic engineering from the City University of Hong Kong in 2001, where he is currently pursuing the M.Phil. degree in power electronics.

His research interests include computer-aided simulation techniques, photovoltaic panels power conversion, control methodologies, and inverter applications.

Mr. Ho received the Simatelex Charitable Foundation Scholarship for two consecutive years during his undergraduate studies.